

Phantom BTZ black holes

B. Eslam Panah^{1,2,3*}, and M. E. Rodrigues^{4,5} [†]

¹ Department of Theoretical Physics, Faculty of Science,

University of Mazandaran, P. O. Box 47416-95447, Babolsar, Iran

² ICRA-Net-Mazandaran, University of Mazandaran, P. O. Box 47416-95447, Babolsar, Iran

³ ICRA-Net, Piazza della Repubblica 10, I-65122 Pescara, Italy

⁴ Faculdade de Ciências Exatas e Tecnologia, Universidade Federal do Pará

Campus Universitário de Abaetetuba, 68440-000, Abaetetuba, Pará, Brazil

⁵ Faculdade de Física, Programa de Pós-Graduação em Física, Brazil

Motivated by the impact of the phantom field (or anti-Maxwell field) on the structure of three-dimensional black holes in the presence of the cosmological constant, we present the first extraction of solutions for the phantom BTZ (A)dS black hole. In this study, we analyze the effect of the phantom field on the horizon structure. Furthermore, we compare the BTZ black holes in the presence of both the phantom and Maxwell fields. Additionally, we calculate the conserved and thermodynamic quantities of the phantom BTZ black holes, demonstrating their compliance with the first law of thermodynamics. Subsequently, we assess the effects of the electrical charge and the cosmological constant on the local stability in the canonical ensemble by considering these fields with respect to the heat capacity. We then investigate the global stability area of the BTZ black holes with phantom and Maxwell fields within the grand canonical ensemble using Gibbs free energy. In this analysis, we evaluate the influence of the electrical charge and the cosmological constant on this area.

I. INTRODUCTION

Black holes are celestial objects characterized by strong gravitational fields and intricate structures. They play an important role in the investigation of theories of gravity. According to the theory of general relativity (GR), a black hole is defined as a region in spacetime encompassed by an event horizon. Hawking further expanded on this concept by demonstrating that the area of an event horizon cannot decrease over time [1]. In this regard, Bekenstein also formulated the concept of black hole entropy [2–4]. It has also been established that there is a correlation between surface gravity and temperature, indicating that surface gravity can be utilized to determine the temperature of a black hole [5]. Hawking proposed a mechanism through which black holes can emit thermal radiation, which is known as Hawking temperature, proportional to their surface gravity. This radiation is caused by quantum fluctuations near the event horizon, which allow for creating virtual particle pairs and observing positive energy flux in distant regions [6]. On the other hand, recent observations have provided compelling evidence supporting the existence of black holes in our universe [7–10]. So, Black holes were regarded as thermodynamic systems, wherein the temperature and entropy are denoted by the surface gravity and area of the black hole horizon, respectively. The study focused on the phase transition of a black hole as a thermodynamic system. Specifically, it was demonstrated that a Hawking-Page phase transition exists between the pure radiation phase and the stable large Schwarzschild black hole phase in AdS space [11, 12]. Additionally, a first-order phase transition, resembling the liquid-gas system, was observed between the small and large black hole phases for charged AdS black holes [13]. Numerous studies have been conducted to explore this phenomenon, considering different types of black holes [14–27].

The first three-dimensional black hole solutions were introduced by Banados, Teitelboim, and Zanelli which are known as BTZ black holes [28]. The significance of BTZ black holes lies in their ability to provide an elegant framework for understanding the interactions of lower-dimensional gravitational systems [29]. They have also been utilized to establish a link with string theory [12], study different thermal properties of black holes [30, 31], and see Refs. [28], for more details. Since then, different theories of gravity to investigate various three-dimensional black hole solutions have been explored in much literature [32–60]. According to the importance of BTZ black holes, we study BTZ black holes.

Observational evidence indicates that our Universe is accelerating, and the concept of dark energy was proposed to explain this accelerated expansion [61–64]. Dark energy can be understood as a field that generates repulsive gravity. One specific type of dark energy, called the phantom field, exists in the Einstein-Maxwell-dilaton system [65] and is studied in relation to ghost branes in string theory [66]. It should be noted that the phantom field may give rise

* email address: eslampah@umz.ac.ir

† email address: esialg@gmail.com

to quantum instabilities [61, 62], presenting a challenge to the theory. However, in Refs. [67, 68] argued that these instabilities can be avoided. Therefore, the phantom field has emerged as a potential candidate for the dark energy model from a theoretical perspective. Given the significance of the phantom field, and particularly its effects on the background of the black hole spacetime, this investigation is important because dark energy will inevitably influence black holes in the Universe. on the other hand, a new black hole solution known as the anti-Reissner-Nordstrom-(A)dS solution or phantom Reissner-Nordstrom-(A)dS black hole solution [69] was extracted in the Einstein-anti-Maxwell theory in the presence of a cosmological constant. These black holes possess a phantom charge, making them fundamentally distinct from the usual Reissner-Nordstrom-(A)dS black holes. Therefore, studying the characteristics of these black holes is of great interest. Historically, Einstein and Rosen proposed the concept of changing $q \rightarrow -q$ in 1935 [70]. They suggested adding a purely imaginary charge, to the Reissner-Nordstrom solution to describe what is known as the quasicharged bridge. The literature extensively discusses phantom black hole solutions in general relativity and other modified theories of gravity [71–75]. So, in this study, our objective is to investigate the phantom BTZ black hole. To achieve this, we will first extract the exact solution of the phantom BTZ black hole. Subsequently, we will analyze other properties, including conserved and thermodynamic quantities, heat capacity, and phase transition.

II. BLACK HOLE SOLUTION

The action of this theory in three-dimensional spacetime is given by

$$\mathcal{I} = \frac{1}{2\kappa^2} \int_{\partial\mathcal{M}} d^3x \sqrt{-g} [R - 2\Lambda + \eta\mathcal{F}], \quad (1)$$

where R and Λ are, respectively, the Ricci scalar curvature and the cosmological constant. The third term is the coupling with the Maxwell field, when $\eta = 1$, or a phantom field of spin 1, when $\eta = -1$. Also, $\mathcal{F} = F_{\mu\nu}F^{\mu\nu}$ is the Maxwell invariant. In addition $F_{\mu\nu} = \partial_\mu A_\nu - \partial_\nu A_\mu$ is the electromagnetic tensor field, and A_μ is the gauge potential. In the above action, $\kappa^2 = 8\pi G$, and G is the Newtonian gravitational constant. Hereafter, we consider $G = c = 1$. Meanwhile, $g = \det(g_{\mu\nu})$ is the determinant of metric tensor $g_{\mu\nu}$.

Making the functional variation of the above action (1), with respect to the gauge field A_μ and the gravitational field $g_{\mu\nu}$, we get the following field equations in the following forms

$$G_{\mu\nu} + \Lambda g_{\mu\nu} = 2\eta \left(\frac{1}{4}g_{\mu\nu}\mathcal{F} - F_\mu^\alpha F_{\nu\alpha} \right), \quad (2)$$

$$\partial_\mu (\sqrt{-g}F^{\mu\nu}) = 0, \quad (3)$$

where $G_{\mu\nu}$ is the Einstein tensor.

We consider a three-dimensional static spacetime in the following form

$$ds^2 = -g(r)dt^2 + \frac{dr^2}{g(r)} + r^2d\varphi^2, \quad (4)$$

where $g(r)$ is the metric function that we have to find it. In order to obtain phantom black hole solutions, we consider a radial electric field which its related gauge potential is given

$$A_\mu = h(r)\delta_\mu^t = (h(r), 0, 0). \quad (5)$$

Using the Maxwell equations (3) with the metric (4), and the mentioned gauge potential (5), we can find the following differential equation by

$$rh''(r) + h'(r) = 0, \quad (6)$$

where the prime and double prime are, respectively, the first and the second derivatives with respect to r . We extract the solution of the equation (6) in the following form

$$h(r) = -q \ln\left(\frac{r}{l}\right), \quad (7)$$

where q is a integration constant which is related to the electric charge. To have logarithmic arguments dimensionless, we introduce l in which is an arbitrary constant with length dimension. Considering the equation (7), the electromagnetic field tensor is given

$$F_{tr} = \partial_t A_r - \partial_r A_t = \frac{q}{r}. \quad (8)$$

Substituting (8) into the equation (2), we get

$$eq_{tt} = eq_{rr} = rg'(r) + 2\Lambda r^2 - 2\eta q^2, \quad (9)$$

$$eq_{\varphi\varphi} = r^2 g''(r) + 2\Lambda r^2 + 2\eta q^2, \quad (10)$$

where eq_{tt} , eq_{rr} and $eq_{\varphi\varphi}$, are components of tt , rr and $\varphi\varphi$ of field equations (2), respectively.

Using the equations (9) and (10), we obtain the metric function in the following form

$$g(r) = -m_0 - \Lambda r^2 + 2\eta q^2 \ln\left(\frac{r}{l}\right), \quad (11)$$

where m_0 is integration constant related to the mass of the black hole.

We calculate the Ricci and Kretschmann scalars for the solution (11) and get them as

$$R = 6\Lambda - \frac{2\eta q^2}{r^2}, \quad (12)$$

$$R_{\alpha\beta\gamma\delta}R^{\alpha\beta\gamma\delta} = 12\Lambda^2 - \frac{8\Lambda\eta q^2}{r^2} + \frac{12\eta^2 q^4}{r^4}, \quad (13)$$

which show that there is a curvature singularity located at $r = 0$, i.e.,

$$\lim_{r \rightarrow 0} R \rightarrow \infty,$$

$$\lim_{r \rightarrow 0} R_{\alpha\beta\gamma\delta}R^{\alpha\beta\gamma\delta} \rightarrow \infty, \quad (14)$$

and also it is finite for $r \neq 0$. The asymptotical behavior of them are given by

$$\lim_{r \rightarrow \infty} R \rightarrow 6\Lambda,$$

$$\lim_{r \rightarrow \infty} R_{\alpha\beta\gamma\delta}R^{\alpha\beta\gamma\delta} \rightarrow 12\Lambda^2, \quad (15)$$

which indicates the spacetime is independent of η , and it will be asymptotically (A)dS.

Horizon Structure: To evaluate the effects of different parameters of these black holes, we plot the metric function (11) versus r in Fig. 1-3. This figure gives us some information about the behavior of horizons. In addition, by studying Figs. 1-3, we can compare the BTZ black holes in the presence of Maxwell and phantom (anti-Maxwell) fields together.

Considering some values of parameters of this solution, we want to investigate the effects of mass, the electrical charge, and the cosmological constant on BTZ black holes in the presence of Maxwell and phantom fields.

Mass: Here, we investigate the impact of the mass parameter on the event horizon. The findings reveal that as the mass increases, both types of black holes become larger. Indeed, the radii of black holes increase as m_0 increases (see Fig. 1). However, there is a significant distinction between charged BTZ black holes in the phantom case in terms of the number of roots. In other words, the phantom BTZ black holes exhibit only one root (or event horizon), as shown in the left panel of Fig. 1. Conversely, BTZ black holes in the presence of the Maxwell field have two roots (inner and outer roots), one root (extremal black holes), and without root (naked singularities), as illustrated in the right panel of Fig. 1. This discrepancy arises from the presence of the phantom effect.

Electrical Charge: Another interesting result is related to the effect of the electrical charge on the event horizon. Our findings show that the higher-charged phantom BTZ black holes have large radii. In other words, by increasing the electrical charge (q), the radius of the phantom black hole increases (see the left panel in Fig. 2). But in the presence of Maxwell field when the electrical charge increases, we first encounter with small BTZ black holes and then the number of roots decreases (see the right panel in Fig. 2).

Cosmological Constant: Phantom BTZ black holes exist for three cases of the cosmological constant ($\Lambda > 0$, $\Lambda < 0$, and $\Lambda = 0$). Indeed, there is an event horizon for BTZ black holes in the presence of a phantom field when the values of the cosmological constant are zero, negative and positive (see the left panel in Fig. 3). But, for $\Lambda > 0$, there are two roots which the smaller root is related to the event horizon and another one is the cosmological horizon.

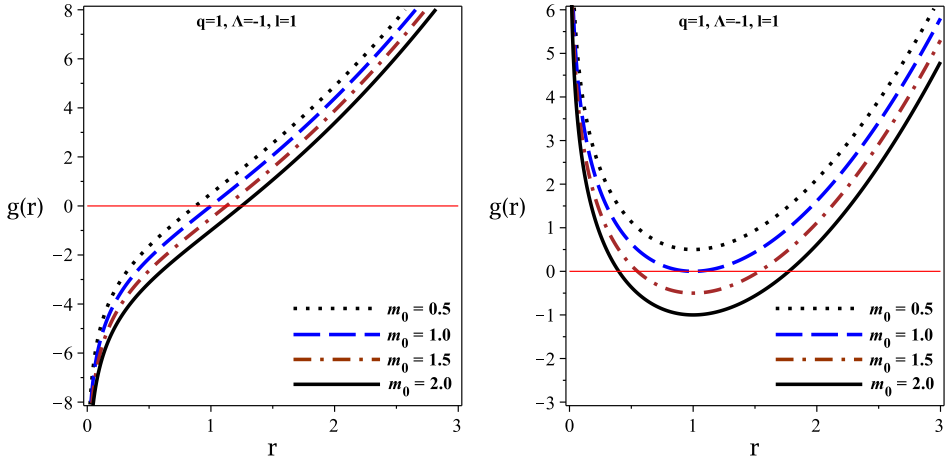


FIG. 1: The metric function $g(r)$ versus r for different values of the mass. Left panels for phantom ($\eta = 1$), and right panels for Maxwell case ($\eta = -1$).

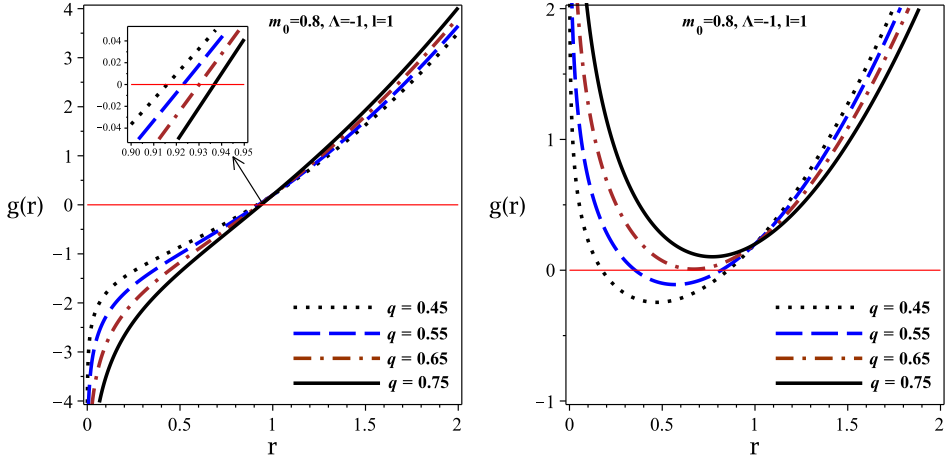


FIG. 2: The metric function $g(r)$ versus r for different values of the electrical charge. Left panels for phantom ($\eta = 1$), and right panels for Maxwell case ($\eta = -1$).

In other words, the small black holes can be exist for $\Lambda > 0$. However, the charged BTZ black holes (Maxwell case) can exist when the value of the cosmological constant is only negative (see the right panel in Fig. 3).

In general, there are three essentially different behaviors of BTZ black holes between Maxwell and phantom fields. i) There is only one root for phantom BTZ black holes. However, the roots of BTZ black holes change in the presence of the Maxwell field. ii) The radius of the phantom BTZ black hole increases with the increase of electric charge, which is different from the Maxwell case. Moreover, the number of roots decreases as the electric charge increases. In fact, BTZ black holes can have two roots (inner and outer roots), one root (extremal black holes) and no root (naked singularities) as the electric charge increases. iii) Phantom BTZ black holes can exist for $\lambda < 0$, $\Lambda > 0$, and $\lambda = 0$. However, the BTZ black hole with Maxwell field only exists in the case $\Lambda < 0$.

III. THERMODYNAMICS

Now, we are interested in to calculate the conserved and thermodynamic quantities of BTZ black holes in the presence of Maxwell and phantom fields to check the first law of thermodynamics.

Using the Hawking temperature, which is given by $T = \frac{\kappa}{2\pi}$ (where κ is the superficial gravity), we can obtain the

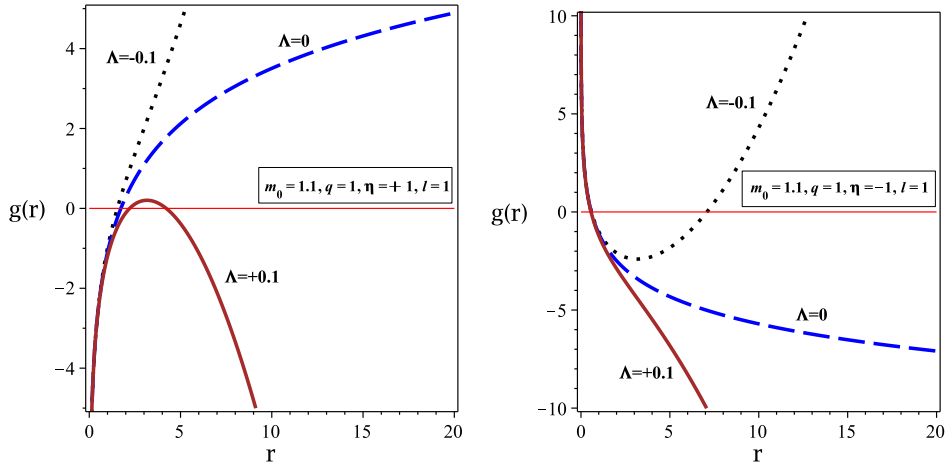


FIG. 3: The metric function $g(r)$ versus r for different values of the cosmological constant. Left panels for phantom ($\eta = 1$), and right panels for Maxwell case ($\eta = -1$).

Hawking temperature of phantom BTZ black holes. For this purpose, by considering $g(r) = 0$, we first express the mass (m_0) in terms of the radius of the event horizon (r_+), the cosmological constant and the charge q in the following form

$$m_0 = 2\eta q^2 \ln\left(\frac{r_+}{l}\right) - \Lambda r_+^2, \quad (16)$$

Then, we calculate the superficial gravity for the mentioned spacetime (4), which leads to

$$\kappa = \frac{g'(r)}{2} \Big|_{r=r_+}, \quad (17)$$

by considering BTZ black holes (11), and by substituting the mass (16) within Eq. (17), one can calculate the superficial gravity as

$$\kappa = \frac{\eta q^2}{r_+} - \Lambda r_+, \quad (18)$$

and so the Hawking temperature leads to

$$T = \frac{\eta q^2}{2\pi r_+} - \frac{\Lambda r_+}{2\pi}. \quad (19)$$

The electric charge of a black hole can be obtained by using the Gauss law in the following form

$$Q = \frac{1}{4\pi} \int_0^{2\pi} F_{tr}(r) \sqrt{g} d\varphi \Big|_{r=r_+} = \frac{q}{2} \quad (20)$$

where $F_{tr}(r) = \frac{q}{r}$, and $g = \det(g_{\mu\nu}) = r^2$.

Using $F_{\mu\nu} = \partial_\mu A_\nu - \partial_\nu A_\mu$, one can find the nonzero component of the gauge potential in which is $A_t = - \int F_{tr}(r) dr$. So, we can get the electric potential (U) at the event's horizon with respect to the reference ($r \rightarrow \infty$) as

$$U = - \int_{r_+}^{+\infty} F_{tr}(r) dr = q \ln\left(\frac{r_+}{l}\right). \quad (21)$$

To obtain the entropy of BTZ black holes, one can use of the area law

$$S = \frac{A}{4}, \quad (22)$$

where A is the horizon area and is defined by

$$A = \int_0^{2\pi} \sqrt{g_{\varphi\varphi}} d\varphi \Big|_{r=r_+} = 2\pi r|_{r=r_+} = 2\pi r_+, \quad (23)$$

where $g_{\varphi\varphi} = r^2$. So, the entropy of BTZ black holes in the presence Maxwell and phantom fields is given by

$$S = \frac{\pi r_+}{2}. \quad (24)$$

Another interesting quantity is related to the total mass of the black hole. To obtain the total mass we use of the Ashtekar-Magnon-Das (AMD) approach [76, 77], and we have

$$M = \frac{m_0}{8}, \quad (25)$$

substituting the mass (16) within the equation (25), yields

$$M = \frac{\eta q^2}{4} \ln \left(\frac{r_+}{l} \right) - \frac{\Lambda r_+^2}{8}. \quad (26)$$

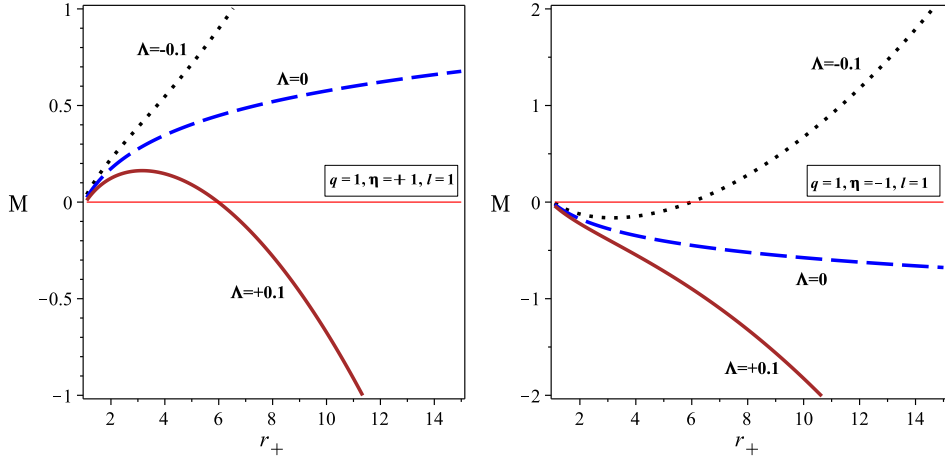


FIG. 4: M versus r_+ for different values of the cosmological constant. Left panels for phantom ($\eta = 1$), and right panels for Maxwell case ($\eta = -1$).

To have a positive mass for the phantom case ($\eta > 0$), the cosmological constant can be positive, negative, or zero, as long as $\Lambda < \frac{2\eta q^2}{r_+^2} \ln \left(\frac{r_+}{l} \right)$ holds. This constraint indicates that the mass of phantom BTZ black holes is always positive when $\Lambda < 0$ and $\Lambda = 0$ (see dotted and dashed lines in the left panel of Fig. 4). However, for $\Lambda > 0$ to have a positive mass, we need to satisfy $\Lambda < \frac{2\eta q^2}{r_+^2} \ln \left(\frac{r_+}{l} \right)$. This reveals that the total mass of black holes cannot be positive for large phantom dS BTZ black holes (see the continuous line in the left panel of Fig. 4). On the other hand, the mass of the Maxwell AdS BTZ black hole with a large radius is positive only for a negative cosmological constant (see the dotted line in the right panel of Fig. 4). This result is consistent with the behavior of the mass (m_0) for the metric function obtained (compare Fig. 3 with Fig. 4).

It is straightforward to show that the conserved and thermodynamics quantities satisfy the first law of thermodynamics in the following form

$$dM = TdS + \eta U dQ, \quad (27)$$

and one can define the intensive parameters conjugate to S and Q . These quantities are the electric potential $(U = \left(\frac{\partial M}{\partial Q} \right)_S)$, and the temperature $(T = \left(\frac{\partial M}{\partial S} \right)_Q)$ which are the same as those calculated for the electric potential (21), and the temperature (19).

IV. THERMAL STABILITY

A. Local Stability

Heat capacity can study a thermodynamic system's local stability in the canonical ensemble context. Therefore, we evaluate the heat capacity to find the local stability for phantom BTZ black holes. Indeed, we study the effect of phantom field on local stability of three-dimensional black holes and compare it with Maxwell field. The heat capacity is given by

$$C_Q = \frac{T}{\left(\frac{\partial T}{\partial S}\right)_Q}. \quad (28)$$

By replacing Eq. (24) in Eq. (19), we can find the Hawking temperature (T) versus S in the following form

$$T = \frac{\eta Q}{S} - \frac{\Lambda S}{\pi^2}, \quad (29)$$

and after some calculation, we can extract the heat capacity of phantom BTZ black holes, which leads to

$$C_Q = \frac{(\Lambda S^2 - \eta \pi^2 Q^2) S}{\Lambda S^2 + \eta \pi^2 Q^2}, \quad (30)$$

We solve C_Q to find the roots of the heat capacity, which are

$$S_{root_1} = \frac{\pi Q \sqrt{\eta \Lambda}}{\Lambda}, \quad \& \quad S_{root_2} = \frac{-\pi Q \sqrt{\eta \Lambda}}{\Lambda}. \quad (31)$$

To have real root, we must respect to the condition $\eta \Lambda > 0$. This imposes the following conditions for phantom and Maxwell fields, which are:

Phantom case ($\eta = 1$): to have a positive value of $\eta \Lambda$ (i.e., $\eta \Lambda > 0$), the cosmological constant must be positive. In this case, $S_{root_1} > 0$ and $S_{root_2} < 0$. Furthermore, there are two roots for the mass. The mass is positive between these roots. Our analysis reveals that the phantom dS BTZ black hole satisfies local stability when it is between S_{root_1} of the heat capacity and the second root of the mass. In other words, medium phantom black holes with a positive value of the cosmological constant (i.e. phantom dS black holes) justify the local stability condition because the mass and the heat capacity are positive (see the hatched area in the left panel of Fig. 5).

Maxwell case ($\eta = -1$): the cosmological constant is negative ($\Lambda < 0$) when we consider the condition $\eta \Lambda > 0$ for the Maxwell case. Therefore, $S_{root_1} < 0$, and $S_{root_2} > 0$. In other words, only S_{root_2} represents the real root of the heat capacity. Our findings indicate that charged AdS BTZ black holes with a large radius (entropy) can be stable. In other words, after the second root of the mass, both the heat capacity and mass are simultaneously positive. Therefore, large BTZ black holes with a negative value of the cosmological constant satisfy local stability (see the hatched area in the right panel of Fig. 5).

To find the heat capacity divergence points, we solve the denominator of Eq. (30) in terms of entropy. We extract them in the following forms

$$S_{div_1} = \frac{\pi Q \sqrt{-\eta \Lambda}}{\Lambda}, \quad \& \quad S_{div_2} = \frac{-\pi Q \sqrt{-\eta \Lambda}}{\Lambda}. \quad (32)$$

To have real root, we must respect to the condition $-\eta \Lambda > 0$. This imposes the following conditions for phantom and Maxwell fields, which are:

Phantom case ($\eta = 1$): by applying the condition $-\eta \Lambda > 0$, the cosmological constant must be negative (i.e., $\Lambda < 0$), and it implies that $S_{div_1} < 0$, and $S_{div_2} > 0$. Therefore, there is a divergence point (S_{div_2}) for the heat capacity. The behavior of the mass and the heat capacity indicate that phantom AdS black holes with a large radius (entropy) satisfy local stability. In other words, large phantom AdS black holes are stable (see the hatched area in the left panel of Fig. 6).

Maxwell case ($\eta = -1$): for this case, the cosmological constant must be positive ($\Lambda > 0$) when considering the condition $-\eta \Lambda > 0$. This condition leads to $S_{div_1} > 0$ and $S_{div_2} < 0$. The results in the right panel of Fig. 6 demonstrate that there is no local stability region for charged BTZ dS black holes, as the mass and heat capacity are not simultaneously positive. In other words, the BTZ black hole in the presence of the Maxwell field with a positive cosmological constant value cannot satisfy local stability.

Briefly, our results reveal that:

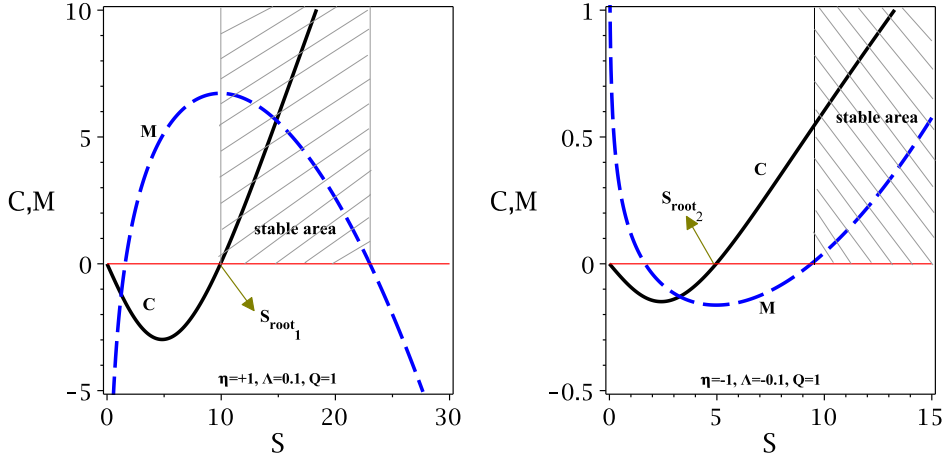


FIG. 5: The heat capacity C_Q and mass (M) versus S for different values of the mass. Left panel for phantom ($\eta = 1$), and right panel for Maxwell case ($\eta = -1$).

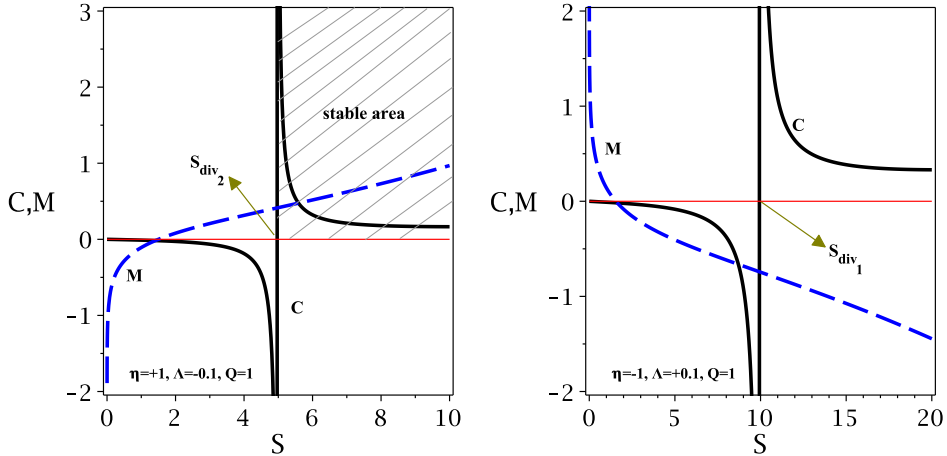


FIG. 6: The heat capacity C_Q and mass (M) versus S for different values of the mass. Left panel for phantom ($\eta = 1$), and right panel for Maxwell case ($\eta = -1$).

i) for $\Lambda > 0$ (dS case), medium phantom BTZ black holes are stable. However, charged BTZ black holes in the presence of the Maxwell field are not stable.

ii) for $\Lambda < 0$ (AdS case), large black holes in the presence of phantom and Maxwell fields exhibit local stability. However, there is a distinct stable region. In other words, phantom BTZ black holes have a larger stable area compared to the Maxwell case.

B. Global Stability

Hawking and Page were the first to suggest studying the global stability of black holes [78]. They proposed that the global stability of a black hole can be assessed in the grand canonical ensemble by calculating the Gibbs free energy. A black hole is deemed globally stable if it possesses negative Gibbs free energy [79, 80]. Here, our objective is to analyze the global stability of phantom BTZ black holes using the Gibbs free energy approach.

It is notable that in the context of the black holes, the Gibbs free energy is defined in the following form

$$G = M(S, Q, \Lambda) - TS - QU. \quad (33)$$

By replacing Eq. (20), and Eq. (24), in Eq. (26), we rewrite the mass of the phantom BTZ black holes as

$$M(S, Q, \Lambda) = \eta Q^2 \ln \left(\frac{2S}{\pi l} \right) - \frac{\Lambda S^2}{2\pi^2}. \quad (34)$$

Using Eqs. (21), (20), (29), and (34) in Eq. (33), we can obtain the Gibbs free energy in the following form

$$G = (\eta - 2) Q^2 \ln \left(\frac{2S}{\pi l} \right) + \frac{\Lambda S^2}{2\pi^2} - \eta Q^2. \quad (35)$$

The global stability areas are deduced from the negative area of the Gibbs free energy (i.e., $G < 0$). We apply the constraint $G < 0$ to find the global stability areas. This constraint imposes the following two conditions:

Condition I: by applying $G < 0$ for phantom BTZ black holes ($\eta = 1$), we find that

$$\Lambda < \frac{2\pi^2 Q^2}{S^2} \left(\ln \left(\frac{2S}{\pi l} \right) + 1 \right), \quad (36)$$

where by adjusting thermodynamic quantities, we can satisfy the above condition. This means that global stability can be achieved for positive, negative, and zero values of the cosmological constant.

Condition II: by considering $G < 0$ for Maxwell BTZ black holes ($\eta = -1$), we can extract the following constraint

$$\Lambda < \frac{2\pi^2 Q^2}{S^2} \left(3 \ln \left(\frac{2S}{\pi l} \right) - 1 \right), \quad (37)$$

so, we can find the global stability areas for $\Lambda > 0$, $\Lambda < 0$, and $\Lambda = 0$ by adjusting the suitable parameters of the above condition.

In order to gain a clear insight into the two conditions mentioned above, we plot the Gibbs free energy versus entropy in Fig. 7 to determine the areas of global stability. Our findings confirm that there is a global stability area for different values of the cosmological constant for BTZ black holes in the presence of both phantom and Maxwell fields. However, the global stability area is more extensive for phantom BTZ black holes compared to Maxwell's case. Furthermore, the global stability area changes with the variation of the electrical charge (Q). These changes are:

- i) In the case of $\Lambda < 0$ (AdS case); the global stability area decreases as the electrical charge increases (see the up panels in Fig. 7).
- ii) In the case of $\Lambda > 0$ (dS case); there exists a critical value for the electrical charge ($Q_{critical}$). For $Q < Q_{critical}$, there is no global stability area, but for $Q > Q_{critical}$, this area appears and increases as the charge increases (see the middle panels in Fig. 7).
- iii) For $\Lambda = 0$; large BTZ black holes satisfy the global stability condition. Furthermore, the global stability area is independent of the electrical charge (see the down panels in Fig. 7).

V. CONCLUSIONS

In this work, the phantom BTZ black hole solutions were extracted in three-dimensional spacetime for the first time. Then, the Ricci and Kretschmann scalars of the obtained solutions were studied to find the curvature singularity. Also, the asymptotical behavior of phantom BTZ black holes was investigated. Our findings indicated that a curvature singularity exists at $r = 0$, and the asymptotical behavior could be (A)dS. To extract different behaviors between the BTZ black holes in the presence of Maxwell and phantom (anti-Maxwell) fields, the effects of different parameters (mass, charged, and the cosmological constant) on the horizon of phantom BTZ black holes were studied. Indeed, phantom BTZ black holes with charged BTZ black holes were compared. Our findings indicated that there were three substantially different behaviors of BTZ black holes between Maxwell and phantom fields, which were: i) There was only one root for phantom (anti-Maxwell) BTZ black holes. However, the roots of BTZ black holes changed in the presence of the Maxwell field. ii) The radius of the phantom BTZ black hole increased with the increase of electric charge, which was different from the Maxwell case. Moreover, the number of roots decreased with increasing electric charge. Our analysis indicated that BTZ black holes can have two roots (inner and outer roots), one root (extremal black holes), and no root (naked singularities) as the electric charge increases. iii) We found that phantom BTZ black holes can exist for $\lambda < 0$, $\Lambda > 0$ and $\lambda = 0$. However, the BTZ black hole with Maxwell field only exists for the case $\Lambda < 0$.

The study focused on obtaining the thermodynamic quantities of BTZ black holes with Maxwell and phantom fields. It was found that these black holes satisfied the first law of thermodynamics. Interestingly, the results showed

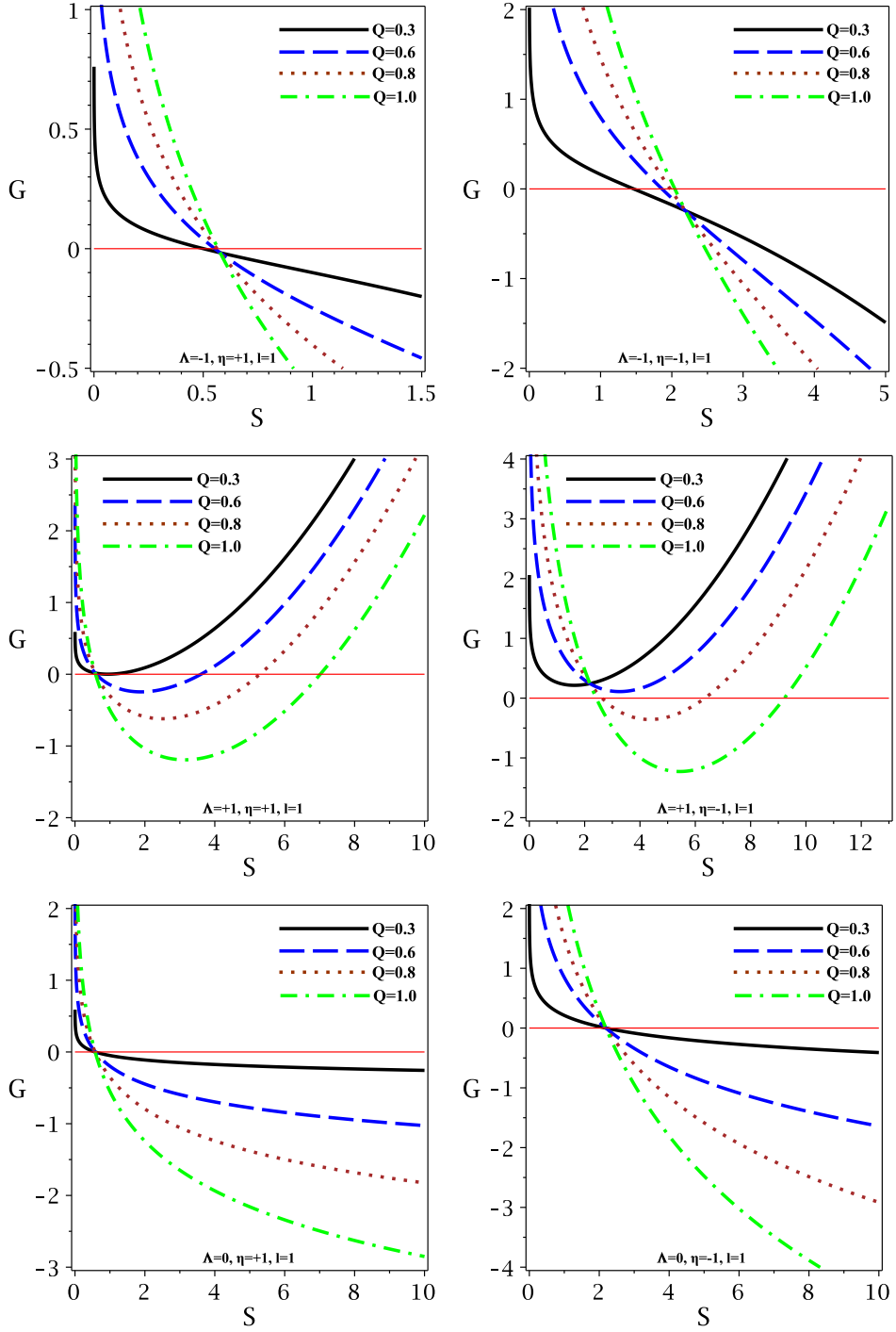


FIG. 7: The Gibbs free energy G versus S for different values of the charge. Left panel for phantom ($\eta = 1$), and right panel for Maxwell case ($\eta = -1$). Up panels for $\Lambda < 0$, middle panels for $\Lambda > 0$, and down panels for $\Lambda = 0$

that the obtained phantom BTZ black holes had a positive mass for all values of the cosmological constant ($\Lambda = 0$, $\Lambda > 0$, and $\Lambda < 0$). Specifically, a constraint was identified in the form of $\Lambda < \frac{2\eta q^2}{r_+^2} \ln \left(\frac{r_+}{l} \right)$, to have a positive mass for the BTZ black holes. This constraint implies that the mass of the phantom BTZ black holes is always positive when $\Lambda < 0$ or $\Lambda = 0$. However, for $\Lambda > 0$, we must respect this constraint. On the other hand, the mass of the Maxwell BTZ black hole was found to be positive only for negative values of the cosmological constant.

The local stability of three-dimensional black holes has been studied in the context of the canonical ensemble using the heat capacity. Our analysis revealed two different behaviors for the heat capacity of the BTZ black hole in the presence of phantom and Maxwell fields. These are as follows:

i) For $\Lambda > 0$ (dS case), medium-sized phantom BTZ black holes were found to be stable. However, charged BTZ black holes in the presence of the Maxwell field were found to be unstable.

ii) For $\Lambda < 0$ (AdS case), large black holes in the presence of phantom and Maxwell fields exhibited local stability. However, there was a distinct stable region. In other words, phantom BTZ black holes had a larger stable area compared to the Maxwell case.

The global stability of BTZ black holes in the presence of phantom and Maxwell fields has been evaluated in the context of the grand canonical ensemble by calculating the Gibbs free energy. Our analysis indicated that the BTZ black holes can satisfy the global stability condition in the presence of phantom and Maxwell fields for all values of the cosmological constant ($\Lambda = 0$, $\Lambda > 0$, and $\Lambda < 0$). However, the global stability area was more extensive for phantom BTZ black holes compared to Maxwell's case. In addition, we have studied the effect of electrical charge on the global stability area. The results revealed that: i) for $\Lambda < 0$, the global stability area decreases as the electrical charge increases. ii) for $\Lambda > 0$ there was a critical value for the electrical charge ($Q_{critical}$), below which there was no global stability area, but above which this area appeared and increased as the charge increased. iii) For $\Lambda = 0$, large BTZ black holes satisfied the global stability condition. Furthermore, the global stability area was independent of the electrical charge.

Acknowledgments

B. Eslam Panah thanks University of Mazandaran..

[1] S. W. Hawking, *Commun. Math. Phys.* **25**, 152 (1972).
[2] J. D. Bekenstein, *Lett. Nuovo Cim.* **4**, 737 (1972).
[3] J. D. Bekenstein, *Phys. Rev. D* **7**, 2333 (1973).
[4] J. D. Bekenstein, *Phys. Rev. D* **9**, 3292 (1974).
[5] J. M. Bardeen, B. Carter, and S. W. Hawking, *Commun. Math. Phys.* **31**, 161 (1973).
[6] S. W. Hawking, *Nature* **248**, 30 (1974).
[7] B. P. Abbott, et al., *Phys. Rev. Lett.* **116**, 061102 (2016).
[8] K. Akiyama, et al., *Astrophys. J. Lett.* **875**, L4 (2019).
[9] K. Akiyama, et al., *Astrophys. J. Lett.* **875**, L6 (2019).
[10] R. Abbott, et al., *Phys. Rev. Lett.* **125**, 101102 (2020).
[11] S. W. Hawking, and D. N. Page, *Commun. Math. Phys.* **87**, 577 (1983).
[12] E. Witten, *Adv. Theor. Math. Phys.* **2**, 505 (1998).
[13] D. Kubiznak, and R. B. Mann, *J. High Energ. Phys.* **07**, 033 (2012).
[14] S. H. Hendi, and M. H. Vahidinia, *Phys. Rev. D* **88**, 084045 (2013).
[15] R. G. Cai, L. M. Cao, L. Li, and R. Q. Yang, *J. High Energ. Phys.* **09**, 005 (2013).
[16] S. W. Wei, and Y. X. Liu, *Phys. Rev. D* **90**, 044057 (2014).
[17] W. Xu, and L. Zhao, *Phys. Lett. B* **736**, 214 (2014).
[18] J. Xu, L. M. Cao, and Y. P. Hu, *Phys. Rev. D* **91**, 124033 (2015).
[19] S. H. Hendi, S. Panahiyan, and B. Eslam Panah, *Int. J. Mod. Phys. D* **25**, 1650010 (2016).
[20] J. X. Mo, G. Q. Li, and Y. C. Wu, *JCAP* **04**, 045 (2016).
[21] Y. G. Miao, and Z. M. Xu, *Eur. Phys. J. C* **77**, 403 (2017).
[22] S. H. Hendi, R. B. Mann, S. Panahiyan, and B. Eslam Panah, *Phys. Rev. D* **95**, 021501(R) (2017).
[23] Y. P. Hu, H. A. Zeng, Z. M. Jiang, and H. Zhang, *Phys. Rev. D* **100**, 084004 (2019).
[24] Y. H. Khan, P. A. Ganai, and S. Upadhyay, *Prog. Theor. Exp. Phys.* **2020**, 103B06 (2020).
[25] B. Eslam Panah, and Kh. Jafarzade, *Gen. Relativ. Gravit.* **54**, 19 (2022).
[26] A. Sood, A. Kumar, J. K. Singh, and S. G. Ghosh, *Eur. Phys. J. C* **82**, 227 (2022).
[27] B. Eslam Panah, *Prog. Theor. Exp. Phys.* **2024**, 023E01 (2024).
[28] M. Banados, C. Teitelboim, and J. Zanelli, *Phys. Rev. Lett.* **69**, 1849 (1992).
[29] E. Witten, [arXiv:0706.3359].
[30] M. Cadoni, and C. Monni, *Phys. Rev. D* **80**, 024034 (2009).
[31] T. Sarkar, G. Sengupta, and B. Nath Tiwari, *J. High Energ. Phys.* **11**, 015 (2006).
[32] R. Emparan, G. T. Horowitz, and R. C. Myers, *J. High Energ. Phys.* **01**, 021 (2000).
[33] S. Carlip, *Class. Quantum Gravit.* **22**, R85 (2005).
[34] Y. S. Myung, Y. W. Kim, T. Moon, and Y. J. Park, *Phys. Rev. D* **84**, 024044 (2011).

[35] E. Frodden, M. Geiller, K. Noui, and A. Perez, *J. High Energ. Phys.* **05**, 139 (2013).

[36] B. Zhang, *Phys. Rev. D* **88**, 124017 (2013).

[37] E. Frodden, M. Geiller, K. Noui, and A. Perez, *J. High Energ. Phys.* **05**, 139 (2013).

[38] F. W. Shu, K. Lin, A. Wang, and Q. Wu, *J. High Energ. Phys.* **04**, 056 (2014).

[39] A. de la Fuente, and R. Sundrum, *J. High Energ. Phys.* **09**, 073 (2014).

[40] G. Gecim, and Y. Sucu, *Gen. Relativ. Gravit.* **50**, 152 (2018).

[41] B. Eslam Panah, et al., *Phys. Rev. D* **98**, 084006 (2018).

[42] S. Kawamoto, K. Nagasaki, and W. Y. Wen, *Prog. Theor. Exp. Phys.* **2018**, 043E01 (2018).

[43] S. T. Hong, Y. W. Kim, and Y. J. Park, *Phys. Rev. D* **99**, 024047 (2019).

[44] B. Eslam Panah, S. Panahiyani, and S. H. Hendi, *Prog. Theor. Exp. Phys.* **2019**, 013E02 (2019).

[45] H. Hassanabadi, et al., *Eur. Phys. J. C* **79**, 936 (2019).

[46] G. Jafari, and H. Soltanpanahi, *J. High Energ. Phys.* **2019**, 195 (2019).

[47] R. Emparan, A. M. Frassino, and B. Way, *J. High Energ. Phys.* **11**, 137 (2020).

[48] E. Verheijden, and E. Verlinde, *J. High Energ. Phys.* **11**, 092 (2021).

[49] B. Narzilloev et al., *Eur. Phys. J. C* **81**, 849 (2021).

[50] R. A. Hennigar, D. Kubiznak, and R. B. Mann, *Class. Quantum Grav.* **38**, 03LT01 (2021).

[51] F. F. Santos, E. F. Capossoli, and H. Boschi-Filho, *Phys. Rev. D* **104**, 066014 (2021).

[52] M. H. Yu, C. Y. Lu, X. H. Ge, and S. J. Sin, *Phys. Rev. D* **105**, 066009 (2022).

[53] B. C. Lutfuoglu, B. Hamil, and L. Dahbi, *Int. J. Mod. Phys. A* **37**, 2250126 (2022).

[54] A. K. Ahmed, S. Shaymatov, and B. Ahmedov, *Phys. Dark Universe* **37**, 101082 (2022).

[55] B. Eslam Panah, *Fortschr. Phys.* **71**, 2300012 (2023).

[56] C. Chen, Q. Pan, and J. Jing, *Phys. Lett. B* **846**, 138186 (2023).

[57] B. Eslam Panah, *Phys. Lett. B* **844**, 138111 (2023).

[58] C. Ding et al., *Eur. Phys. J. C* **83**, 573 (2023).

[59] B. Eslam Panah, M. Khorasani, and J. Sedaghat, *Eur. Phys. J. Plus* **138**, 728 (2023).

[60] B. Eslam Panah, K. Jafarzade, and A. Rincon, *Gen. Relativ. Gravit.* **56**, 46 (2024).

[61] R. R. Caldwell, *Phys. Lett. B* **545**, 23 (2002).

[62] S. Hannestad, *Int. J. Mod. Phys. A* **21**, 1938 (2006).

[63] Y. F. Cai, E. N. Saridakis, M. R. Setare, and J.-Q. Xia, *Phys. Rept.* **493**, 1 (2010).

[64] J. Dunkley et al., (WMAP collaboration), *Astrophys. J. Suppl.* **180**, 306 (2009).

[65] G. Clement, J. C. Fabris, and M. E. Rodrigues, *Phys. Rev. D* **79**, 064021 (2009).

[66] T. Okuda, and T. Takayanagi, *J. High Energ. Phys.* **06**, 062 (2006).

[67] S. Nojiri, and S. D. Odintsov, *Phys. Lett. B* **562**, 147 (2003).

[68] F. Piazza, and S. Tsujikawa, *JCAP* **04**, 004 (2004).

[69] D. F. Jardim, M. E. Rodrigues, and M. J. S. Houndjo, *Eur. Phys. J. Plus* **127**, 123 (2012).

[70] A. Einstein, and N. Rosen, *Phys. Rev.* **48**, 73 (1935).

[71] K. A. Bronnikov, and J. C. Fabris, *Phys. Rev. Lett.* **96**, 251101 (2006).

[72] G. Clement, J. C. Fabris, and M. E. Rodrigues, *Phys. Rev. D* **79**, 064021 (2009).

[73] M. Azreg-Ainou, G. Clement, J. C. Fabris, and M. E. Rodrigues, *Phys. Rev. D* **83**, 124001 (2011).

[74] B. Eslam Panah, and M. E. Rodrigues, *Eur. Phys. J. C* **83**, 237 (2023).

[75] Kh. Jafarzade, B. Eslam Panah, and M. E. Rodrigues, *Class. Quantum Grav.* **41**, 065007 (2024).

[76] A. Ashtekar, and A. Magnon, *Class. Quantum Gravit.* **1**, L39 (1984).

[77] A. Ashtekar, and S. Das, *Class. Quantum Gravit.* **17**, L17 (2000).

[78] S. Hawking, and D. N. Page, *Commun. Math. Phys.* **87**, 577 (1983).

[79] R. G. Cai, and A. Wang, *Phys. Rev. D* **70**, 064013 (2004).

[80] M. Dehghani, and M. R. Setare, *Phys. Rev. D* **100**, 044022 (2019).